Available online at www.sciencedirect.com
ScienceDirect
Journal of Power Sources 177 (2008) 685–689
JOURNAL OF POWER SOURCES
www.elsevier.com/locate/jpowsour

Short communication

Al-substituted α-cobalt hydroxide synthesized by potentiostatic deposition method as an electrode material for redox-supercapacitors

Vinay Gupta [a,b,*], Shubhra Gupta [a], Norio Miura [a]

[a] *Art, Science and Technology Center for Cooperative Research, Kyushu University, Kasuga-shi, Fukuoka 816-8580, Japan*
[b] *Japan Science and Technology Agency, Kawaguchi-shi, Saitama 332-0012, Japan*

Received 20 August 2007; received in revised form 19 October 2007; accepted 26 October 2007
Available online 12 November 2007

Abstract

Al-substituted α-cobalt hydroxide was prepared by a potentiostatic deposition process at −1.0 V (vs. Ag/AgCl) onto stainless steel electrodes by using a mixed aqueous solution of cobalt nitrate and aluminum nitrate. Their structure and surface morphology were studied by using X-ray diffraction analysis, energy dispersive X-ray spectroscopy and scanning electron microscopy. The SEM images showed changes in the nanostructure of α-cobalt hydroxide by the addition of Al. Galvanostatic charge–discharge curves showed a drastic improvement in the capacitive characteristics of α-cobalt hydroxide, with a specific energy increase from 11.3 to 18.7 Wh kg^{-1} by the substitution of just 8 at.% Al, and a specific capacitance of 843 F g^{-1} between 0 and 0.4 V. The cycle stability data suggest no significant changes in the discharge characteristics of α-cobalt hydroxide by the addition of Al.

Keywords: Cobalt hydroxide; Aluminum hydroxide; Potentiostatic deposition; Specific capacitance; Supercapacitor

1. Introduction

Supercapacitors are attracting significant attention as energy efficient, eco-friendly, high-power, high-energy devices. Their long cycle life, excellent safety and eco-friendly nature are highly advantageous in offering alternatives to fossil-fuel, and thus they can contribute significantly in controlling global warming [1–6]. Their potential applications include vehicles, such as cars, buses, trains, etc., and portable devices, such as mobile phones, laptop computers, memory devices, etc.

Significant advancements have been achieved in the last few years in supercapacitor technology. However there are two main areas that need to be addressed: (1) the ability to tailor supercapacitor properties to meet the very specific operational requirements of individual applications; and (2) the need to drive down the costs of supercapacitors to levels commensurate with the financial viability of the applications in which they are to be used [5,6].

Metal oxide electrodes are very promising as supercapacitors due to their high power density, energy density, mass density and cycle stability as compared to carbon or polymer electrodes. Since the discovery of RuO_2 as a high-capacitance material [7–9], several metal oxides such as vanadium oxide [10] nickel oxide [11], cobalt oxide [12] and manganese oxide [13], have been studied as electrode active materials for electrochemical capacitors. The interest in other oxides has been mainly due to the high cost of RuO_2; however, they have thus far failed to match the specific capacitance of RuO_2 [10–12].

Recently, a number of publications [14–22] have shown that metal hydroxides can have higher capacitance than metal oxides, due to their layered structure, which can result in high utilization of the electrode material. Recently, we have shown that a specific capacitance higher than that of RuO_2 can be achieved in the case of electrochemically deposited $Co(OH)_2$ [22]. However, the charge–discharge characteristics of $Co(OH)_2$ have indicated that most of the specific energy is associated with the low poten-

* Corresponding author at: Art, Science and Technology Center for Cooperative Research, Kyushu University, Kasuga-shi, Fukuoka 816-8580, Japan. Tel.: +81 92 583 7886; fax: +81 92 583 7886.
E-mail address: vinay@astec.kyushu-u.ac.jp (V. Gupta).

0378-7753/$ – see front matter © 2007 Elsevier B.V. All rights reserved.
doi:10.1016/j.jpowsour.2007.10.091

tial range. Therefore, an increase in the specific energy in the high potential range would be of significant importance for the practical applicability of such materials. This requires the partial substitution of the Co ion in the cobalt hydroxide lattice by other metal ions. Al is an attractive candidate to synthesize such a stabilized structure due to its trivalent nature [19,23].

In this paper, Al–Co layered double hydroxides (LDHs) have been prepared by the substitution of Al^{3+} ions into the cobalt hydroxide lattice by the potentiostatic deposition method. It was observed that the characteristics of the Al–Co LDHs can be controlled by varying the amount of substituted Al in the cobalt hydroxide lattice.

2. Experimental

Analytical grade chemicals ($Co(NO_3)_2{\cdot}6H_2O$, $Al(NO_3)_3{\cdot}9H_2O$ and 1 M KOH) and research grade stainless-steel (SS, grade 304, 0.2 mm thick) were used for the Al–Co LDH preparations. In the initial measurements, we used SS electrodes of several sizes from 1 cm × 1 cm to 6 cm × 8 cm. It was found that the supercapacitive characteristics are almost independent of the electrode size. The deposition was homogenous in all cases. However, in this work, the area of the SS favored for deposition was 6 cm × 8 cm from the viewpoint of practical applications. The SS was polished with emery paper to a rough finish, washed free of abrasive particles and then air-dried. An electrochemical cell was assembled in a three-electrode configuration in which the counter electrode was platinum (Pt), the reference electrode was Ag/AgCl (saturated KCl solution), and the working electrode was SS. $Al(NO_3)_3{\cdot}9H_2O$ was added in 0.005, 0.10 and 0.20 M concentrations in the aqueous solution of 0.1 M $Co(NO_3)_2{\cdot}6H_2O$ to prepare Al-substituted α-cobalt hydroxide. The deposition was carried out by potentiostatic deposition at a potential of −1.0 V versus Ag/AgCl. The details of the potentiostatic deposition method are given elsewhere [22].

The deposited electrodes were washed in distilled water by using a magnetic paddle in a beaker and then dried in an oven at 50 °C overnight. The weight of the deposit was measured by means of a micro-balance (Sartorius, BP211D) with an accuracy of 0.01 mg. The weights of all deposited Co–Ni LDHs were ∼10 mg. The deposition was controlled by monitoring the coulombic charge. The elemental analysis was carried out by the use of an energy dispersive X-ray (EDX) spectrometer (EDAX, Horiba EX-220SE) coupled to a scanning electron microscope (Hitachi, S3000-N). The microstructure of the electrode materials was evaluated by the use of a field emission scanning electron microscope (FE-SEM, JEOL, JSM-6340F). The X-ray diffraction patterns were obtained by the use of an X-ray diffractrometer (XRD, RIGAKU, R1NT2100) with Cu Kα radiation (λ = 1.5406 Å) operating at 40 kV, 20 mA. The TG/DTA curves were obtained by using an SII TG/DTA analyzer (SII, Model 3200). All electrochemical depositions and capacitive measurements were performed by the use of a potentiostat (AUTOLAB®, Eco Chemie, PGSTAT 30). The capacitive characterization was performed in 1 M KOH electrolyte.

Table 1
EDX analysis of Al contents in $Co(OH)_2$ as compared to Al contents in the initial molar solutions of $Co(NO_3)_2{\cdot}6H_2O$ and $Al(NO_3)_3{\cdot}9H_2O$

Sample no.	Al content in solution [Al/(Co+Al)] (%)	Al content in sample [Al/(Co+Al)] (at.%)
1	5	8
2	10	25
3	20	59

3. Results and discussion

The Al contents in the initial solution as well as in the deposited Al–Co LDHs, obtained by means of EDX analysis, are given in Table 1. It can be seen that the content of substituted Al is proportional to that in the initial solution. In the following text, the Al–Co LDHs are abbreviated as Al_xCo_{1-x}LDHs, with $x = 0.08$, 0.25 and 0.59. From the remaining balance oxygen, the hydrated water content was estimated to be 3 at.%.

Fig. 1(a) shows the XRD patterns of $Co(OH)_2$ and Al_xCo_{1-x}LDHs ($x = 0.08$, 0.25 and 0.59). The patterns of $Co(OH)_2$ in Fig. 1(a) comprise four broad peaks, appearing at 2θ values of 11.3° (7.84 Å), 22.6° (3.92 Å), 32.9° (2.72 Å) and 58.8° (1.57 Å). The effect of trivalent Al^{3+} can be noticed in the X-ray diffraction patterns. As the at.% of Al in $Co(OH)_2$ was increased, the positions of the diffraction peaks shifted slightly. The most noticeable change was observed in the case of the (0 0 1) diffraction peak, which shifted to a higher d value. For the

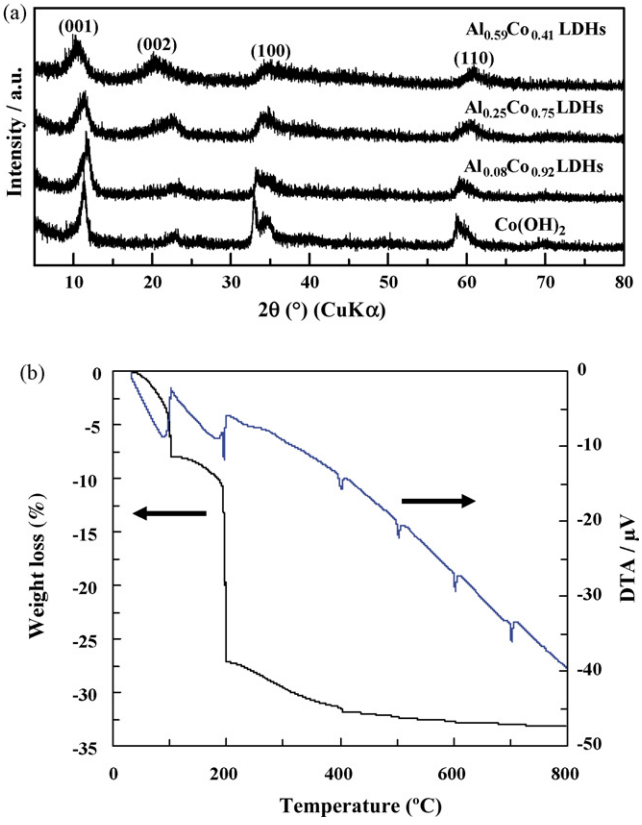

Fig. 1. (a) XRD patterns of the $Al_{0.25}Co_{0.75}$LDHs and (b) TG/DTA curves of the $Al_{0.25}Co_{0.75}$LDHs.

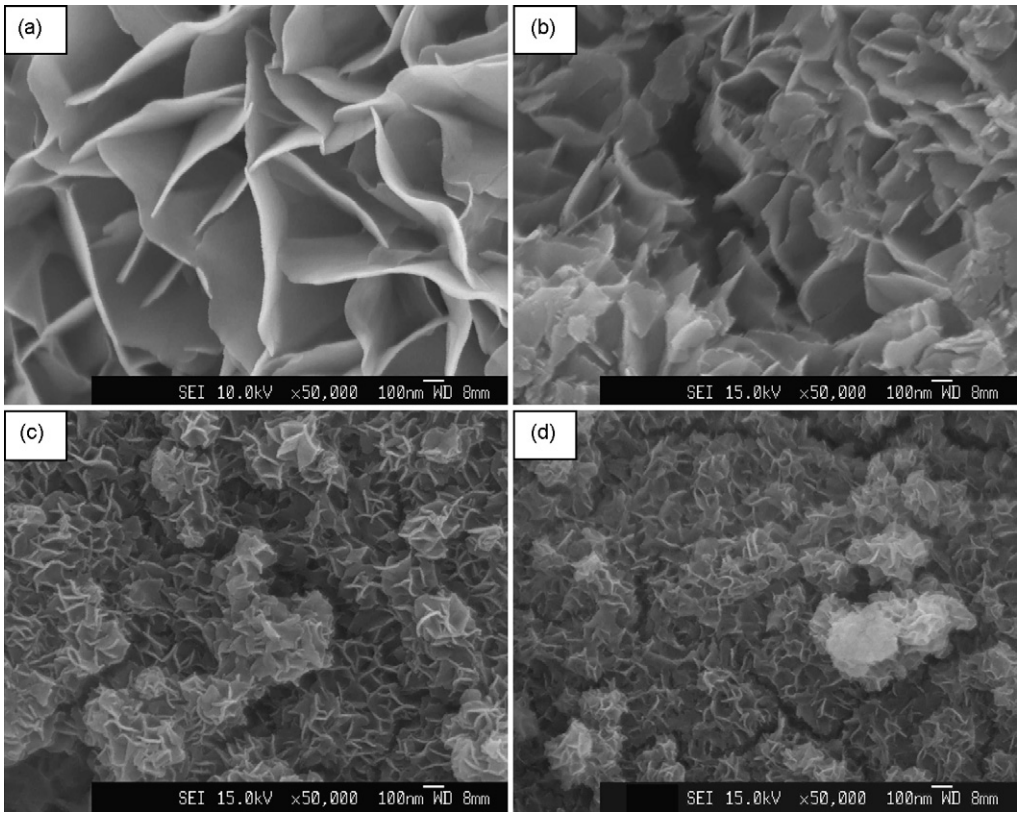

Fig. 2. SEM images of the Al_xCo_{1-x}LDHs with x values of (a) 0, (b) 0.08, (c) 0.25 and (d) 0.59.

$Al_{0.59}Co_{1-0.41}$LDHs, the $d_{(0\,0\,1)}$ value was 8.49 Å (0 0 ℓ). However, the substitution of Al did not affect the crystal structure of $Co(OH)_2$ significantly. Fig. 2(b) shows the TG/DTA curves of the deposited $Al_{0.25}Co_{0.75}$ LDH in air. The TG curve showed an initial weight loss of ~8 wt.% at around 100 °C, which is due to the desorption of physically adsorbed water, and thereafter, the main weight loss of ~21 wt.%, in the temperature range of 180–300 °C, may be due to the decomposition of the $Al_{0.25}Co_{0.75}$ LDH into the respective oxides. Since the loss of hydrated water occurs in a similar temperature range, its amount could not be estimated. The TG/DTA curves were similar for all of the deposits.

The SEM images of the deposited Al_xCo_{1-x}LDHs ($x = 0.08$, 0.25 and 0.59) are shown in Fig. 2. The microstructure of the pure $Co(OH)_2$ is shown in Fig. 2(a), in which nano-sheets of ~10 nm thickness and sizes of several hundred nanometers were observed. When the amount of Al substitution in $Co(OH)_2$ was 8 at.% ($Al_{0.08}Co_{0.92}$LDH), a decrease in the sizes of the nanosheets was observed (Fig. 2b). For Al substitution of 25 at.% ($Al_{0.25}Co_{0.75}$LDH), the structure was converted to the nanometer scale (Fig. 2c). No further change was observed upon increasing Al substitution up to 59 at.% ($Al_{0.59}Co_{0.41}$LDH), as shown in Fig. 2(d).

Fig. 3(a) shows the CV curves of $Co(OH)_2$, $Al_{0.08}Co_{0.92}$LDH, $Al_{0.25}Co_{0.75}$LDH and $Al_{0.59}Co_{0.41}$LDH in 1 M KOH electrolyte at the scan rate of 10 mV s^{-1} in the potential range of −1.0 to +0.45 V. $Co(OH)_2$ shows very strong redox peaks ($x = 0$) due to the following Faradaic reactions [21]:

$$Co(OH)_2 + OH^- \leftrightarrows CoOOH + H_2O + e^- \quad (1)$$

$$CoOOH + OH^- \leftrightarrows CoO_2 + H_2O + e^- \quad (2)$$

The profiles of the CV curves changed significantly to rectangular shape after 8 at.% substitution of Al ($x = 0.08$). The nature of the CV curve for Al-doped $Co(OH)_2$ in Fig. 3(a) suggests a significant increase of the capacitance in the higher potential range, as marked by arrows, which increased further as the amount of substituted Al was increased to 25 at.% ($x = 0.25$). For the 59 at.% Al-substituted $Co(OH)_2$ ($x = 0.59$), a significant decrease in the redox capacitance in the lower potential range was observed.

Fig. 3(b) shows the charge–discharge (CD) curves for $Co(OH)_2$, $Al_{0.08}Co_{0.92}$LDH, $Al_{0.25}Co_{0.75}$LDH and $Al_{0.59}Co_{0.41}$LDH in 1 M KOH electrolyte at 1 A g^{-1} current in the potential range of 0–0.4 V. One can observe redox characteristics in the CD curves of $Co(OH)_2$ ($x = 0$) that are directly related to the redox peaks in the CV curves (Fig. 3a). The profiles of the CD curves changed significantly after the 8 at.% substitution of the Al ($x = 0.08$) and was close to that of an ideal triangular shape (marked by arrows). This is due to an increase in the capacitance in the higher potential range. This is supported by the CV curve in Fig. 3(a). Such an enhancement in the capacitance may be due to an increase in the surface area, as seen in the SEM image in Fig. 2(b). The specific capacitances for $Co(OH)_2$ and 8 wt.% Al-substituted $Co(OH)_2$

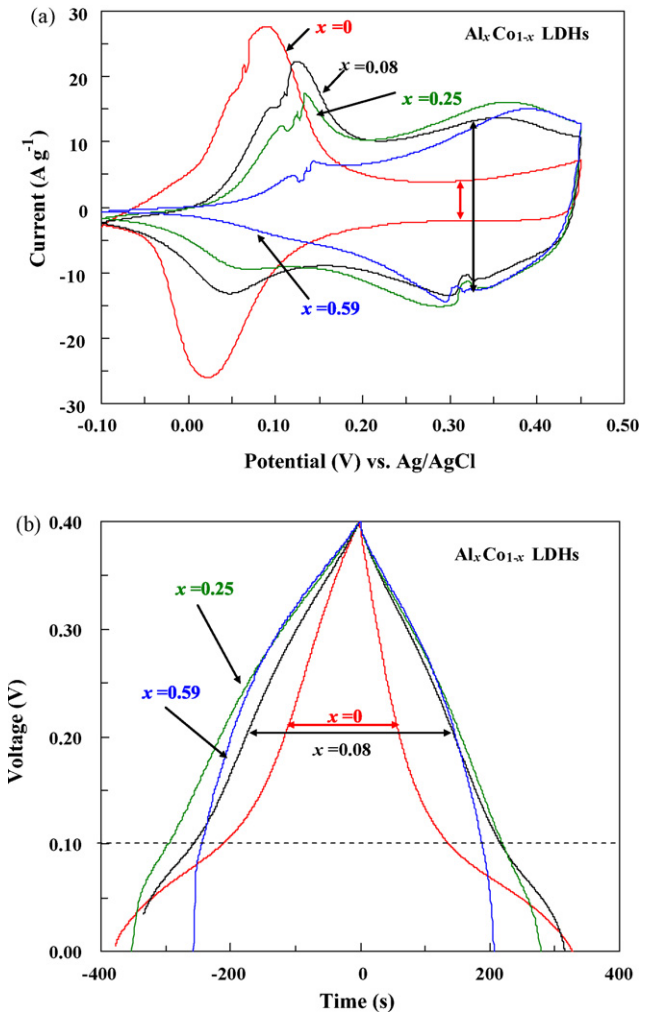

Fig. 3. (a) Cyclic voltammograms at 10 mV s^{-1} and (b) charge–discharge curves of the Al_xCo_{1-x}LDHs at 1 A g^{-1}.

were 840 and 843 F g^{-1}, respectively. The profiles of the CD curves remained the same, even after 25 at.% substitution of Al ($x = 0.25$); however, the specific capacitance decreased to 706 F g^{-1}. The specific capacitance decreased to 520 F g^{-1} for 59 wt.% Al-substituted $Co(OH)_2$ ($x = 0.59$).

The specific energy (SE) can be calculated from the charge–discharge cycling data by using the following relationship:

$$\mathrm{SE\,(Wh\,kg^{-1})} = \frac{I\,(\mathrm{A}) \times t\,(\mathrm{s}) \times \Delta E\,(\mathrm{V})}{m\,(\mathrm{kg})} \quad (3)$$

where I (A), t (s) and m (kg) are discharge current in amperes, discharge time in seconds and mass of active electrode material in kilograms, respectively, and ΔE is the discharge potential in volts. The most important advantage of the Al substitution is the enhancement in the specific capacitance and specific energy in the potential range of 0.1–0.4, as shown in Fig. 4(a) and (b). This leads to a 42% increase in the specific capacitance (Fig. 4a) and a 64% increase in the specific energy (Fig. 4b) of $Co(OH)_2$ by just 8 at.% substitution of Al, which is marked by a large circle in Fig. 4. Also, both the specific capacitance and the specific

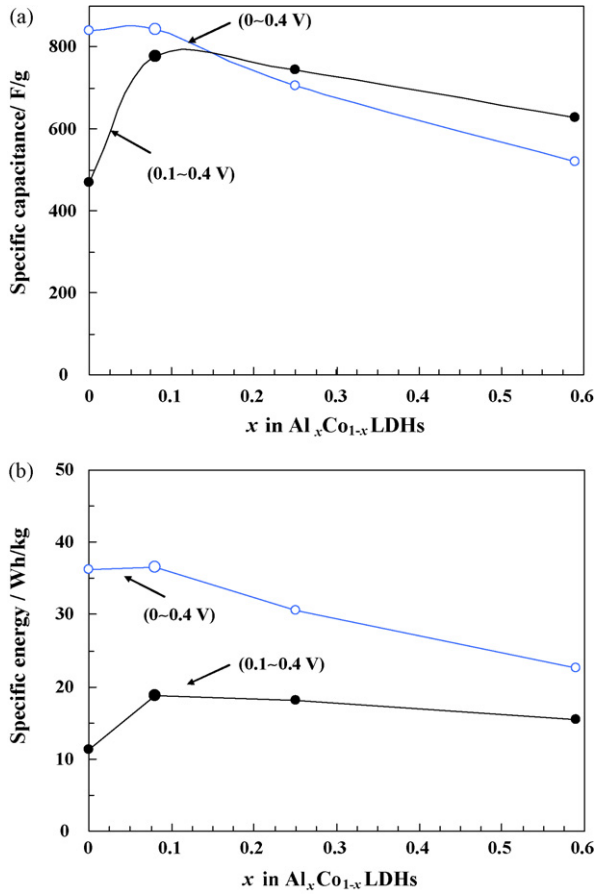

Fig. 4. (a) Specific capacitance and (b) specific energy values of the Al_xCo_{1-x}LDHs as a function of x in Al_xCo_{1-x}LDHs.

energy of the Al-substituted $Co(OH)_2$ samples were higher than those of $Co(OH)_2$ in the 0.1–0.4 potential range. Therefore, by the substitution of just 8 at.% Al, a nearly ideal supercapacitive behavior was obtained, without any significant change in the specific capacitance, and thus the prime objective of this study was achieved. This is of significant importance from the point of view of practical applications of $Co(OH)_2$. In addition, the cycle life test indicates that Al-substituted $Co(OH)_2$ is very stable.

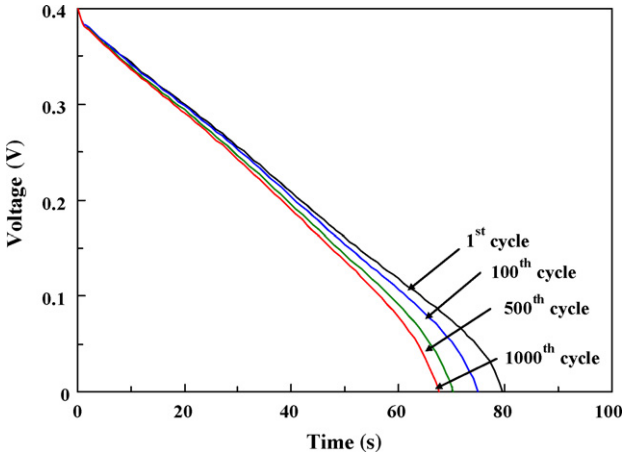

Fig. 5. The cyclic stability data of $Al_{0.08}Co_{0.92}$LDHs at 4 A g^{-1}.

The cycling data for 8 wt.% Al-substituted $Co(OH)_2$ is shown in Fig. 5, up to 1000 cycles.

In conclusion, Al-substituted cobalt hydroxides were synthesized by the potentiostatic deposition method. Drastic changes in the nanostructure as well as a significant improvement in the capacitive characteristics were observed. In the case of pure $Co(OH)_2$, most of its capacitance lies in the potential range below 0.1 V. Also the charge–discharge behavior is far from ideal rectangular one. So it is difficult to use in practical supercapacitor. By the doping of Al, the charge–discharge behavior become closer to ideal rectangular behavior and a significant increase in the specific energy is observed. Therefore, Al_xCo_{1-x}LDHs have superior characteristics as compared to $Co(OH)_2$. The present study indicates that the capacitive characteristics of the $Co(OH)_2$ can be modified by the substitution, and therefore its properties can be tailored for specific applications.

Acknowledgement

The present work was supported by the Japan Science and Technology (JST) Agency through the Core Research for Evolutionary Science and Technology (CREST) program under the project "Development of advanced nanostructured materials for energy conversion and storage."

References

[1] B.E. Conway, Electrochemical Supercapacitors, Kluwer Academic/Plenum Publishers, New York, 1999, p. 1.
[2] L.T. Lam, R. Louey, J. Power Sources 158 (2006) 1140.
[3] J.R. Miller, Electrochim. Acta 52 (2006) 1703.
[4] T.A. Centeno, F. Stoeckli, in: V. Gupta (Ed.), Recent Advances in Supercapacitors, Transworld Research Network, Kerala, India, 2006, p. 57.
[5] J.R. Miller, Electrochemistry 75 (2007) 563.
[6] K. Naoi, Electrochemistry 75 (2007) 564.
[7] S. Trasatti, G. Buzzanca, J. Electroanal. Chem 29 (1971) A1.
[8] T.C. Wen, C.C. Hu, J. Electrochem. Soc. 139 (1992) 2158.
[9] J.P. Zheng, P.J. Cygan, T.R. Jow, J. Electrochem. Soc. 142 (1995) 2699.
[10] W. Dong, J.S. Sakamoto, B. Dunn, Sci. Technol. Adv. Mater. 1 (2003) 3.
[11] K.W. Nam, K.B. Kim, J. Electrochem. Soc. 149 (2002) A 346.
[12] V. Srinivasan, J.W. Weidner, J. Power Sources 108 (2002) 15.
[13] T. Shinomiya, V. Gupta, N. Miura, Electrochim. Acta 51 (2006) 4412.
[14] R.S. Jayashree, P.V. Kamath, J. Mater. Chem. 9 (1999) 961.
[15] C.C. Hu, C.Y. Cheng, Electrochem. Solid State Lett. 5 (2002) A43.
[16] J.H. Park, O.O. Park, K.H. Shin, C.S. Jin, J.H. Kim, Electrochem. Solid State Lett. 5 (2002) H7.
[17] T.N. Ramesh, M. Rajamathi, P.V. Kamath, Solid State Ionics 5 (2003) 751.
[18] L. Cao, F. Xu, Y.Y. Liang, H.L. Li, Adv. Mater. 16 (2004) 1853.
[19] Y. Wang, W. Yang, S. Zhang, D.G. Evans, X. Duan, J. Electrochem. Soc. 152 (2005) A2130.
[20] D.D. Zhao, S.S. Bao, W.J. Zhou, H.L. Li, Electrochem. Commun. 9 (2007) 869.
[21] Y.Y. Liang, S.J. Bao, H.L. Li, J. Solid State Electrochem. 11 (2007) 571.
[22] V. Gupta, N. Miura, Electrochem. Commun. 9 (2007) 2316.
[23] Y. Wang, W. Yang, J. Yang, Electrochem. Solid State Lett. 10 (2007) A233.